

Supplementary Materials

Hierarchically constructed NiO with improved performance for catalytic transfer hydrogenation of biomass-derived aldehydes

Jian He,^{a,b} Monia Runge Nielsen,^c Thomas Willum Hansen,^c Song Yang,^{b,*} Anders Riisager^{a,*}

^a Centre for Catalysis and Sustainable Chemistry, Department of Chemistry, Technical University of Denmark, DK-2800 Kgs. Lyngby, Denmark.

^b State Key Laboratory Breeding Base of Green Pesticide & Agricultural Bioengineering, Key Laboratory of Green Pesticide & Agricultural Bioengineering, Ministry of Education, State-Local Joint Laboratory for Comprehensive Utilization of Biomass, Center for Research & Development of Fine Chemicals, Guizhou University, Guiyang 550025, PR China.

^c Center for Electron Nanoscopy, Technical University of Denmark, DK-2800 Kgs. Lyngby, Denmark.

(Summary of Content: 20 pages, 12 figures, 5 tables and 1 scheme)

Figure and Table Captions:

Figure S1. NH₃-TPD profiles of (a) commercial NiO nanoparticles, (b) NiO(P)-300, (c) NiO(P)-400 and (d) NiO-300.

Figure S2. CO₂-TPD profiles of (a) commercial NiO nanoparticles, (b) NiO(P)-300, (c) NiO(P)-400 and (d) NiO-300.

Figure S3. TEM image of commercial NiO nanoparticles.

Figure S4. FAOL selectivity as a function of particle size of different catalysts.

Figure S5. (a) GC chromatograms of reaction mixtures (from GC-MS) obtained from the CTH of FF to FAOL over NiO(P)-300 catalyst after 1 h at different reaction temperature and (b) MS chromatogram of 2-(diisopropoxymethyl)furan.

Figure S6. (a) Kinetic profiles of FF to FAOL conversion by the NiO(P)-300 catalyst (X: FF conversion), (b) Arrhenius plot of formation of FAOL from FF.

Figure S7. FAOL yield profiles of the reaction solution with NiO(P)-300 catalyst or without catalyst (separated after 1 h).

Figure S8. XPS of Ni 2p_{3/2} of (a) fresh, (b) used and (c) regenerated NiO(P)-300 catalyst.

Figure S9. Pictures of (a) fresh, (b) used and (c) regenerated NiO(P)-300 catalyst.

Figure S10. ¹H NMR spectrum (in CD₃Cl) of the as-synthesized FAOL from gram-scale experiment.

Figure S11. ¹H NMR spectrum (in CD₃Cl) of as-prepared IPL.

Figure S12. GC chromatograms of reaction mixtures obtained from the one-pot conversion of FF to IPL over (a) NiO(P)-300 and Amberlyst 15 and (b) NiO(P)-300 and H-Beta catalyst.

Table S1. Comparison of the activity of NiO(P)-300 with other heterogeneous catalysts in the production of FAOL from FF with alcohols in hydrogenation donor reaction systems.

Table S2. Detail data of kinetic studies and calculated activation energy for the CTH of FF over NiO(P)-300.

Table S3. Catalytic performance of NiO(P)-300 in 2-BuOH at different reaction temperature.

Table S4. One-pot conversion of FF to IPL with NiO(P)-300 and other acid catalysts.

Table S5. Effect of acid or base additive on the CTH of FF to FAOL over NiO(P)-300.

Scheme S1. Gram-scale CTH of FF to FAOL over NiO(P)-300 catalyst.

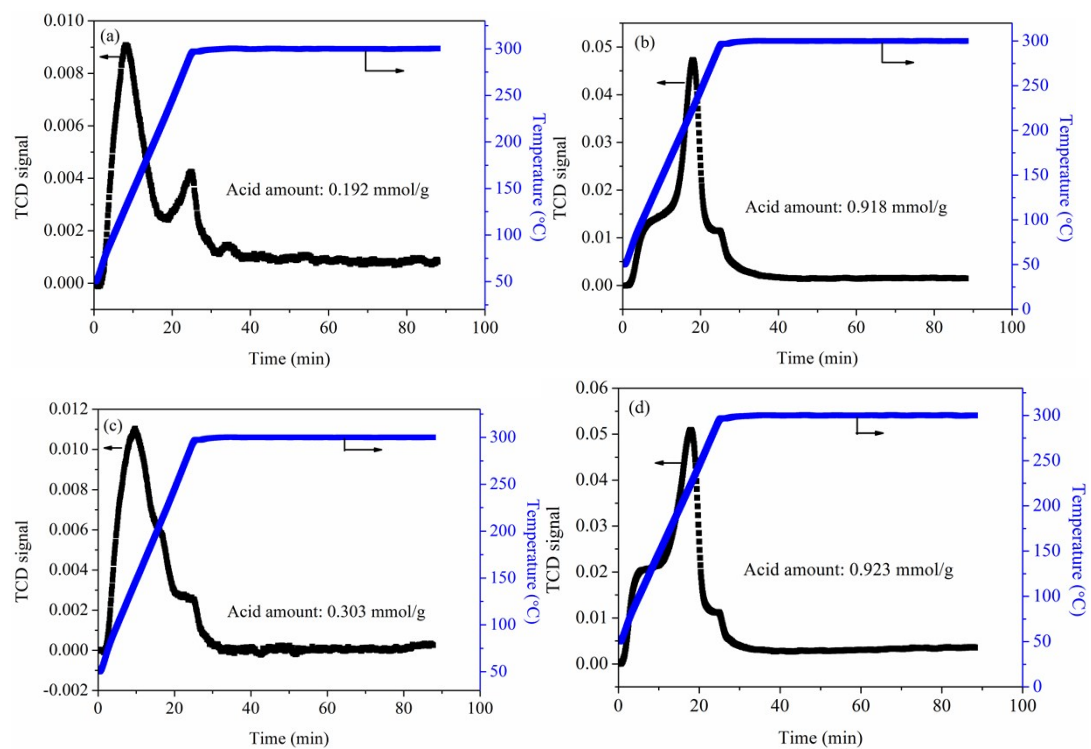


Figure S1. NH_3 -TPD profiles of (a) commercial NiO nanoparticles, (b) NiO(P)-300, (c) NiO(P)-400 and (d) NiO-300.

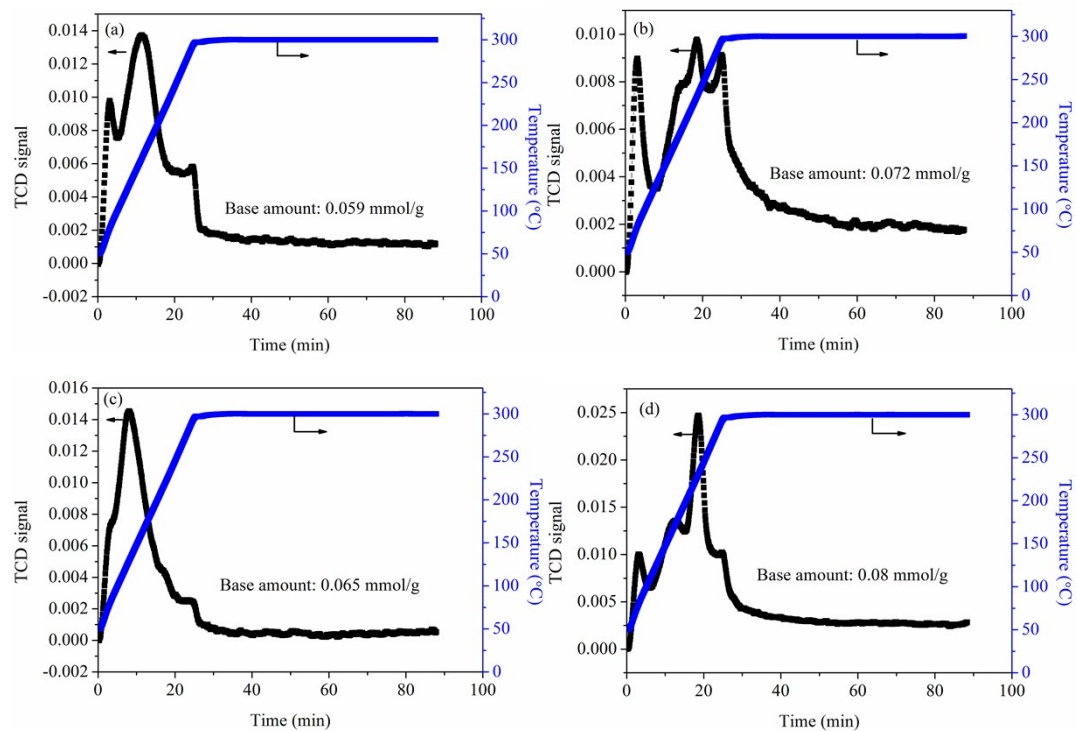


Figure S2. CO₂-TPD profiles of (a) commercial NiO nanoparticles, (b) NiO(P)-300, (c) NiO(P)-400 and (d) NiO-300.

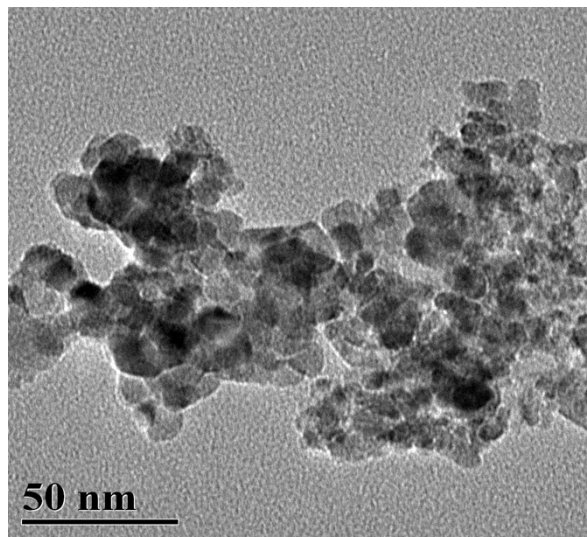


Figure S3. TEM image of commercial NiO nanoparticles.

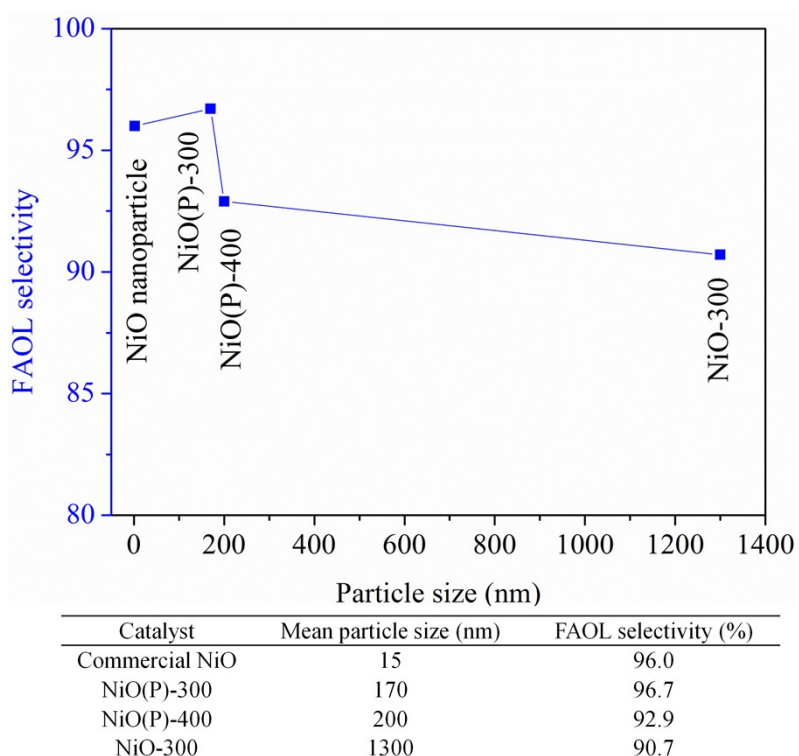


Figure S4. FAOL selectivity as a function of particle size of different catalysts. Reaction conditions: 1 mmol FF, 0.02 g catalyst, 5 mL 2-propanol, 120 °C, 1 h. Mean particle size was determined from TEM measurement.

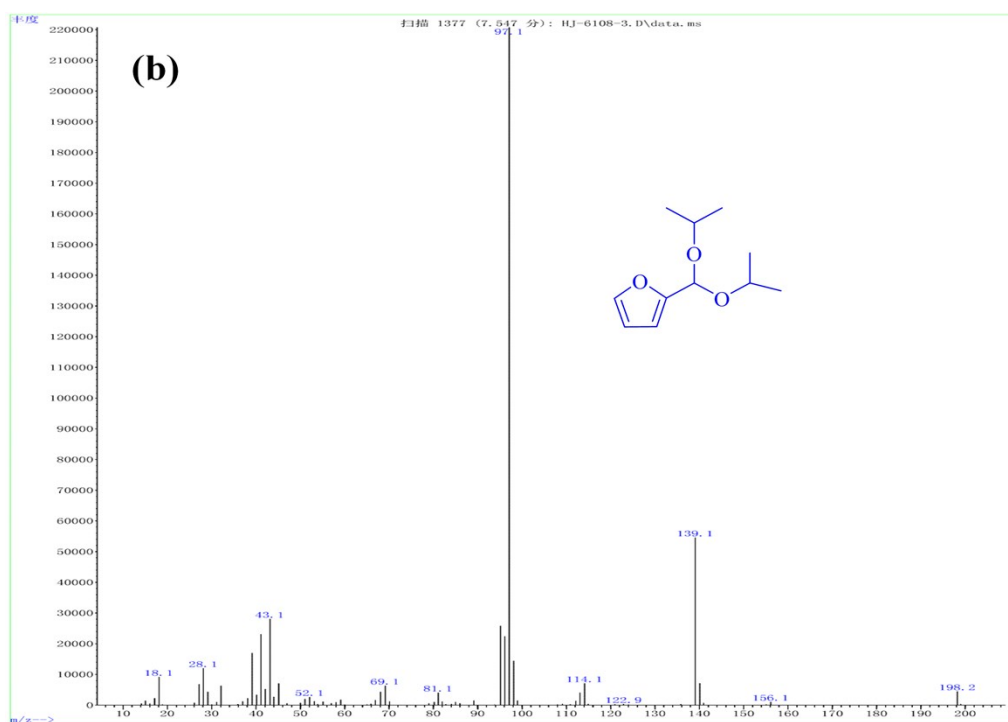
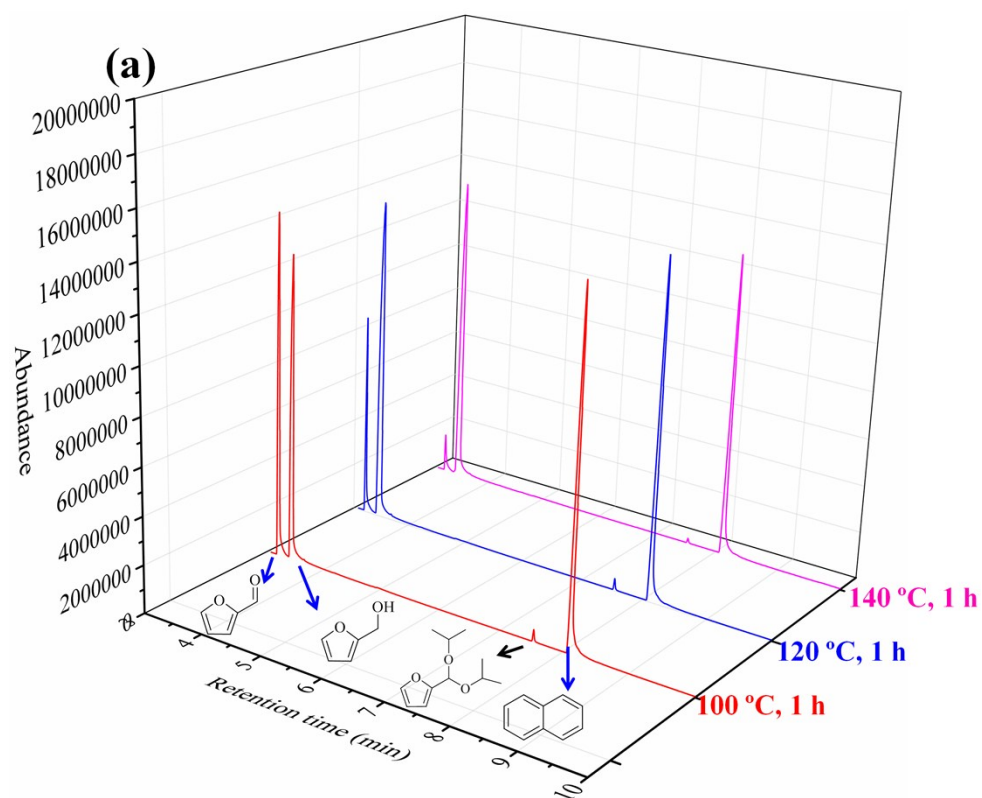


Figure S5. (a) GC chromatograms of reaction mixtures (from GC-MS) obtained from the CTH of FF to FAOL over NiO(P)-300 catalyst after 1 h at different reaction temperature and (b) MS chromatogram of 2-(diisopropoxymethyl)furan.

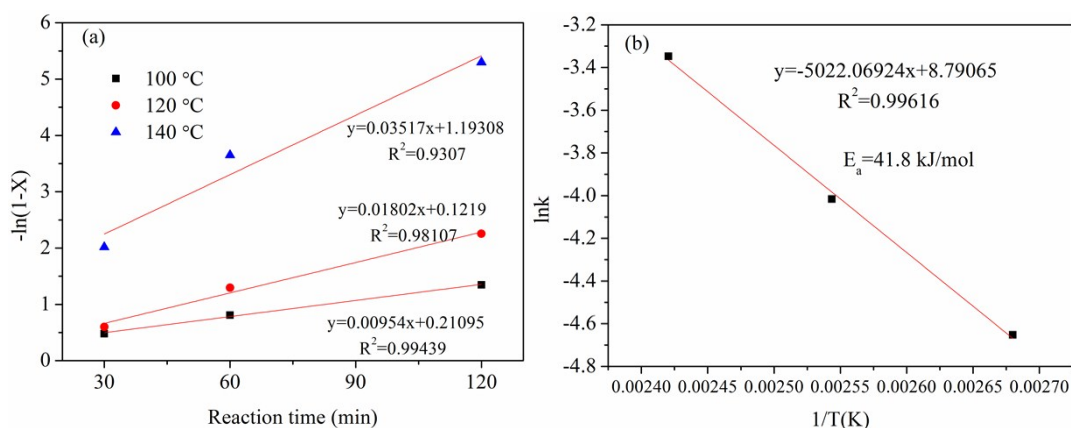


Figure S6. (a) Kinetic profiles of FF to FAOL conversion by the NiO(P)-300 catalyst (X: FF conversion), (b) Arrhenius plot of formation of FAOL from FF.

In the applied reaction system, the concentration of 2-propanol didn't affect the reaction kinetics due to excess use of 2-propanol. Thus, the transfer hydrogenation of FF is assumed to be a pseudo-first order process. The reaction rate can be expressed as the following equation as a first-order rate to FF concentration:

$$-d[FF]/dt = k[FF] = d[FAOL]/dt$$

[FF] and [FAOL] represent concentrations of FF and FAOL, respectively, and k is the rate constant of FF hydrogenation at certain temperature.

After the integral calculation, the above equation is transformed into the following equation:

$$-\ln(1-X) = kt + C$$

Herein, X is FF conversion whereas t and C are reaction time and an arbitrary constant, respectively.

In order to calculate the rate constant (k), values of $-\ln(1-X)$ versus reaction time were plotted at different reaction temperature, and the reaction rate constants (k) calculated from the slopes of the plot in Fig. S6a.

The activation energy (E_a) can be calculated by the following Arrhenius equation:

$$\ln k = -(E_a/R) \cdot (1/T) + \ln A$$

The value of E_a was calculated on the basis of the linear of $\ln k$ versus $1/T$ as displayed in Fig. S6b.

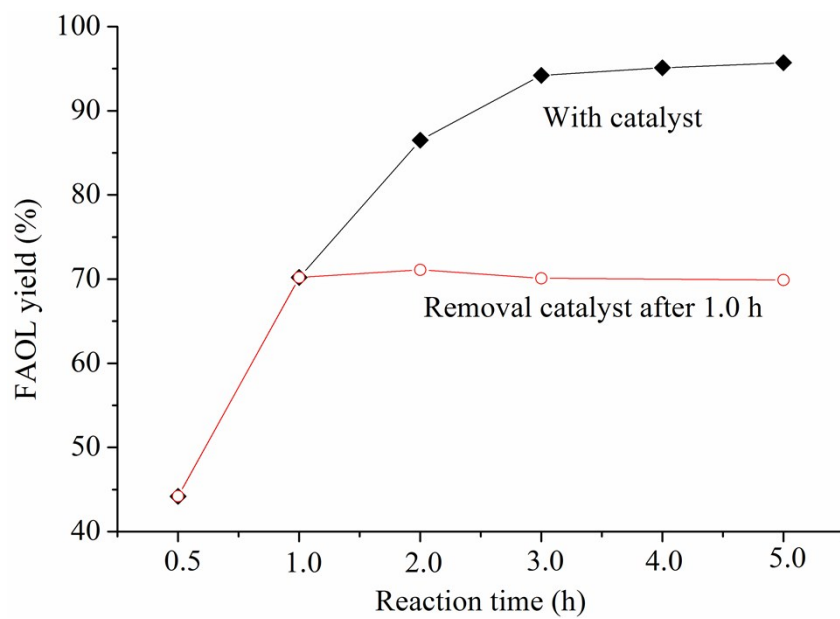


Figure S7. FAOL yield profiles of the reaction solution with NiO(P)-300 catalyst or without catalyst (separated after 1 h). Reaction conditions: 1 mmol FF, 5 mL 2-propanol, 0.02 g NiO(P)-300, 120 °C.

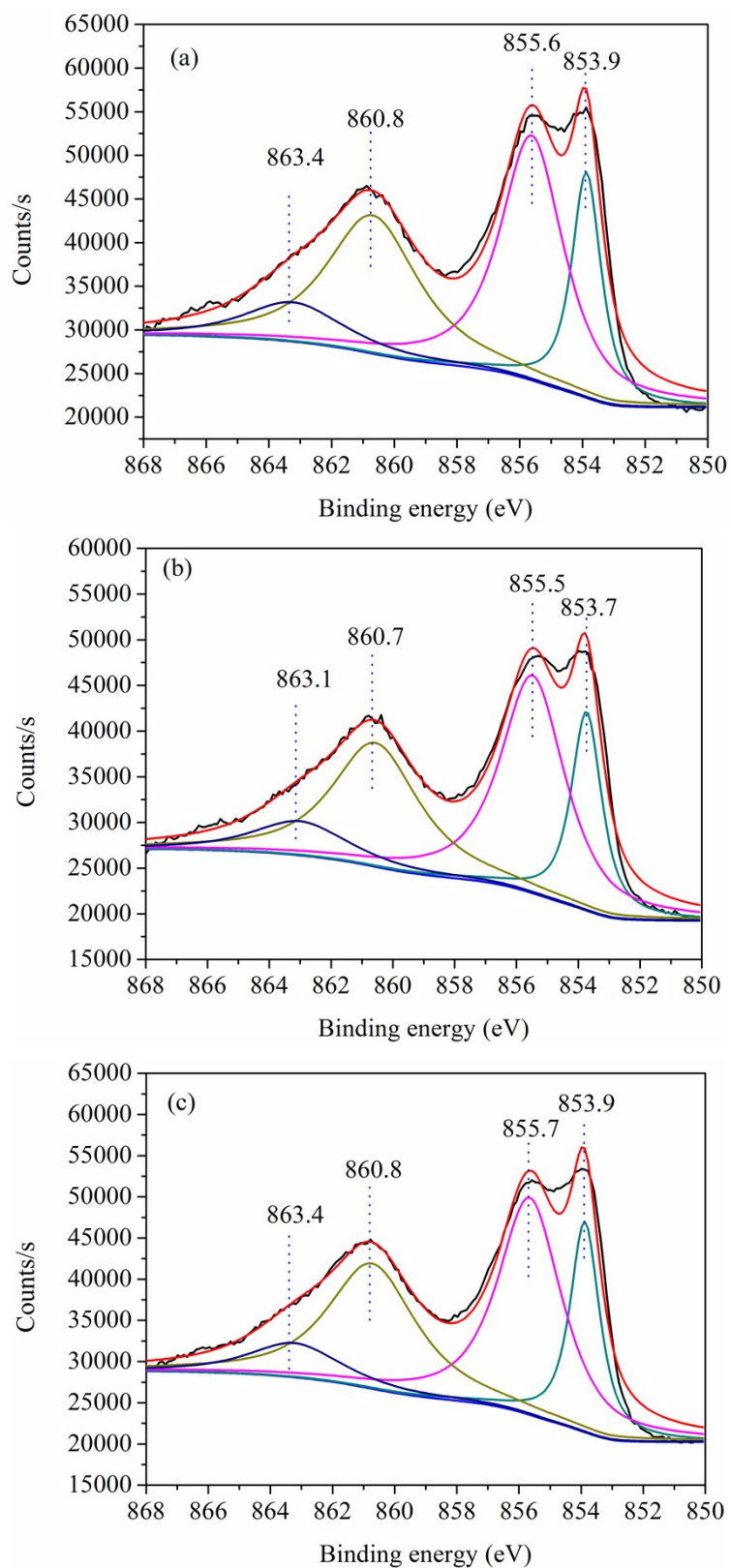


Figure S8. XPS of Ni 2p_{3/2} of (a) fresh, (b) used and (c) regenerated NiO(P)-300 catalyst.

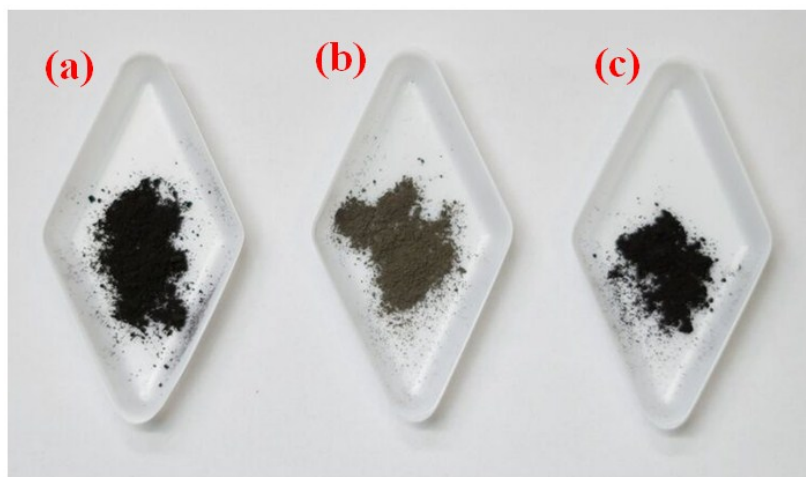


Figure S9. Pictures of (a) fresh, (b) used and (c) regenerated NiO(P)-300 catalyst.

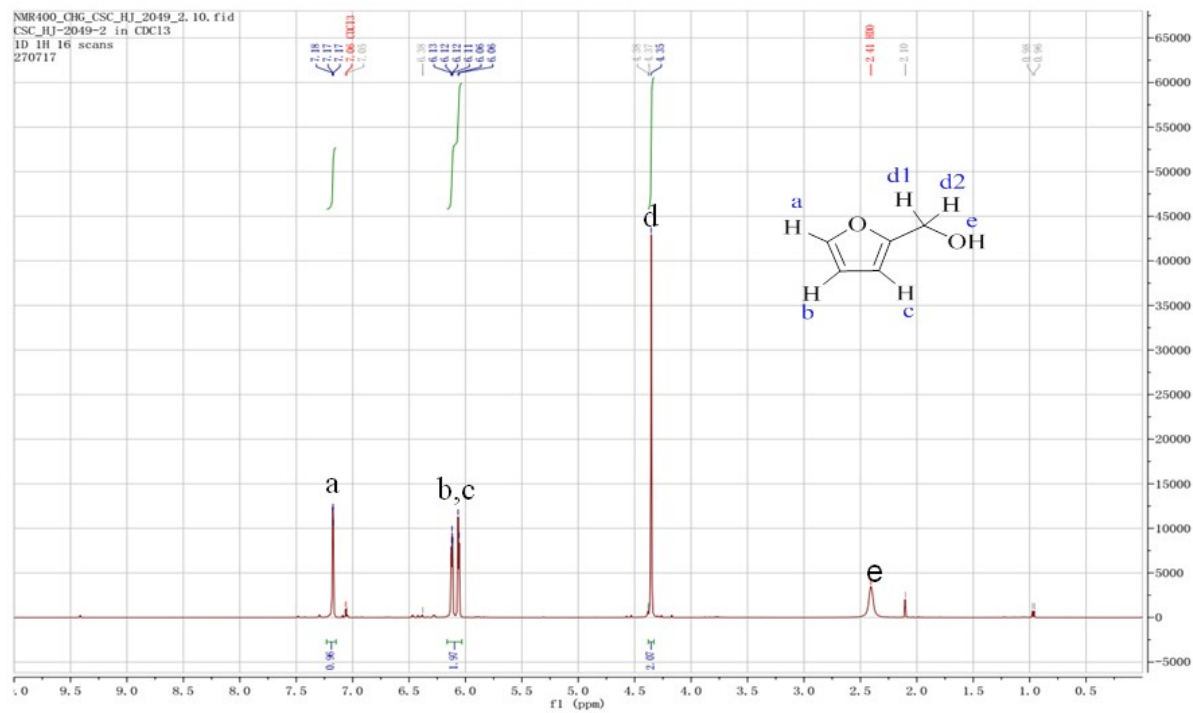


Figure S10. ^1H NMR spectrum (in CD_3Cl) of the as-synthesized FAOL from gram-scale experiment.

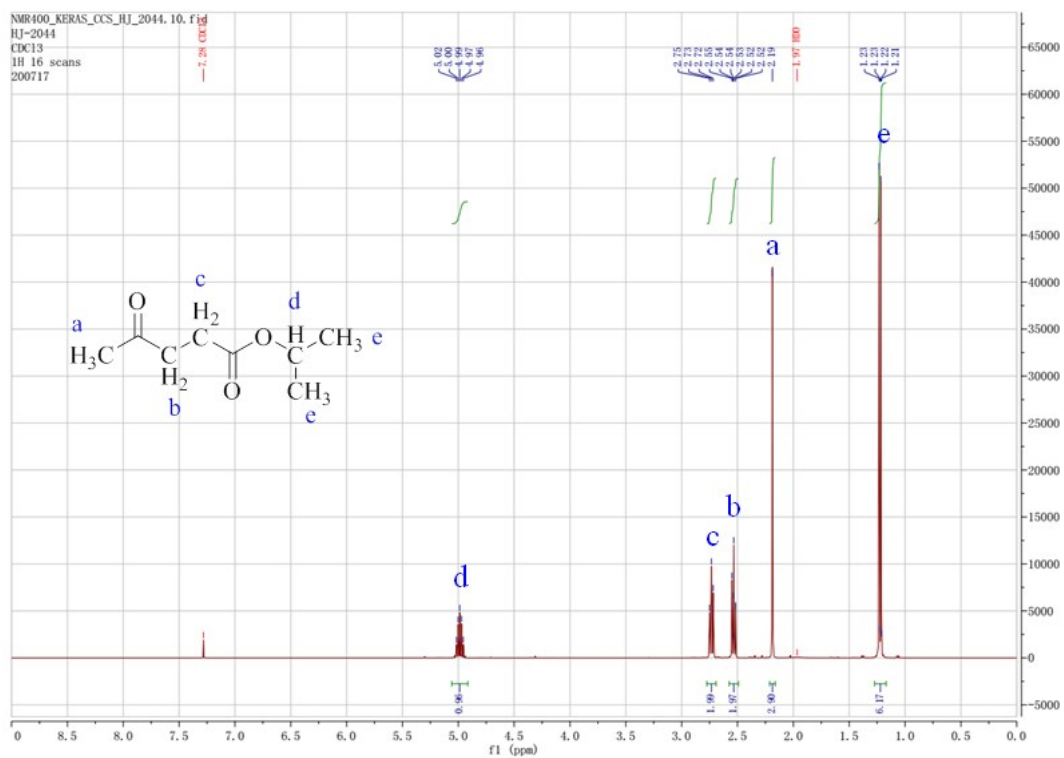


Figure S11. ^1H NMR spectrum (in CD_3Cl) of as-prepared IPL.

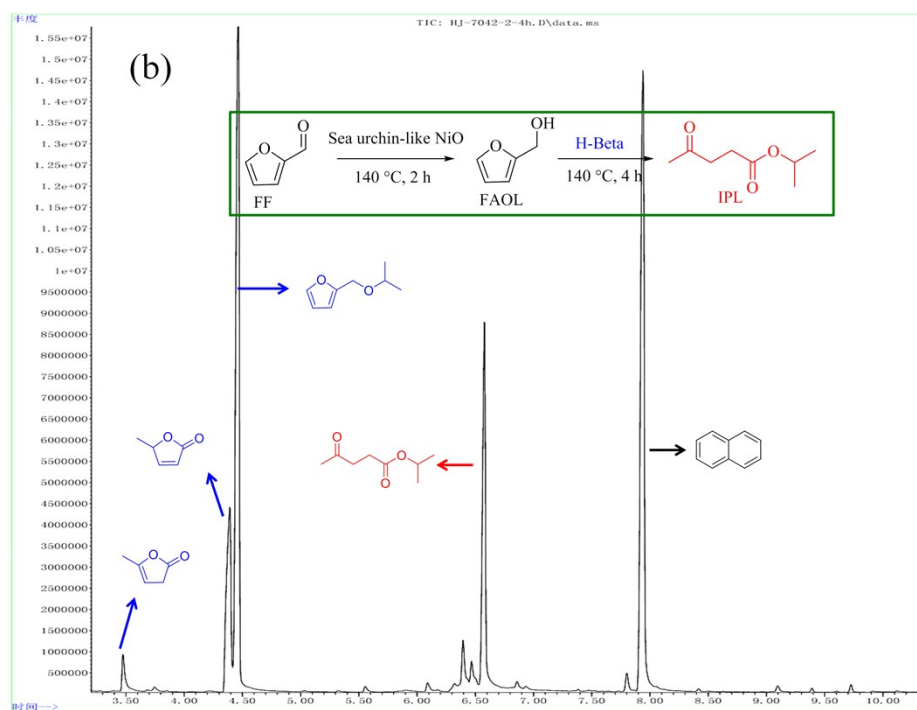
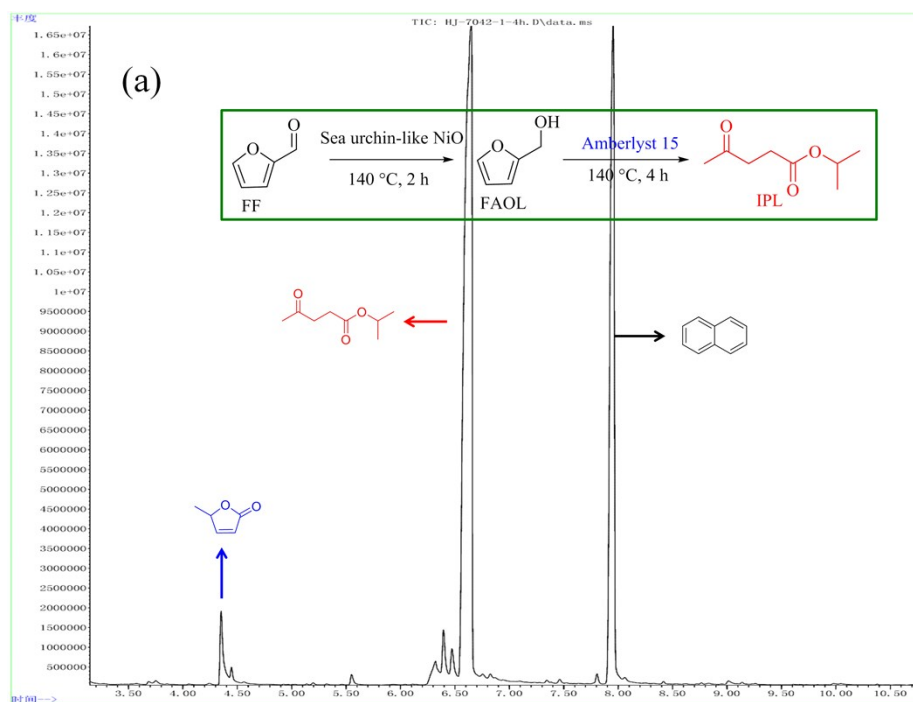


Figure S12. GC chromatograms of reaction mixtures obtained from the one-pot conversion of FF to IPL over (a) NiO(P)-300 and Amberlyst 15 and (b) NiO(P)-300 and H-Beta catalyst.

Table S1. Comparison of the activity of NiO(P)-300 with other heterogeneous catalysts in the production of FAOL from FF with alcohols in hydrogenation donor reaction systems.

Catalyst	H-donor	Cat. amount ^a (%)	T (°C)	t (h)	Conv (%)	Yield (%)	Sel. (%)	E _a (kJ/mol)	Ref.
Co ₃ O ₄ /MC ^b	2-Propanol	52.1	120	8	100	>97	>97	-	[S1]
Co-Ru/C	Benzyl alcohol	28.9	150	12	98	98	100	58	[S2]
γ-Fe ₂ O ₃ @HAP ^c	2-Propanol	41.6	180	10	96.2	91.7	95.3	47.69	[S3]
MgO	2-Propanol	10.0	170	5	>99.9	74	74	-	[S4]
Fe-L1/C-800	2-Butanol	104.2	160	15	91.6	76.0	83	-	[S5]
Ni-Cu/Al ₂ O ₃	2-Propanol	22.3	200	4	95.43	95.41	>99	-	[S6]
Ru/C+DyCl ₃	2-Propanol	52.1	180	3	100	97	97	-	[S7]
ZrPN	2-Propanol	41.7	140	2	98	98	>99	70.5	[S8]
Pd/Fe ₂ O ₃	2-Propanol	33.3	150	7.5	66	37	56.1	46.8	[S9]
NiO (sea urchin)	2-Propanol	20.8	120	3	97.3	94.2	96.8	41.8	This work

^a Relative to initial mass of FF. ^b MC = mesoporous carbon; ^c HAP = hydroxyapatite.

[S1] Wang, G. H.; Deng, X.; Gu, D.; Chen, K.; Tüysüz, H.; Spliethoff, B.; Bongard, H.; Weidenthaler, C.; Schmidt, W.; Schüth, F. *Angew. Chem. Int. Ed.*, **2016**, *55*, 11101-11105.

[S2] Gao, Z.; Yang, L.; Fan, G.; Li, F. *ChemCatChem*, **2016**, *8*, 3769-3779.

[S3] Wang, F.; Zhang, Z. *ACS Sustain. Chem. Eng.*, **2017**, *5*, 942-947.

[S4] Biradar, N. S.; Hengne, A. M.; Sakate, S. S.; Swami, R. K.; Rode, C. V. *Catal. Lett.*, **2016**, *146*, 1611-1619.

[S5] Li, J.; Liu, J.; Zhou, H.; Fu, Y. *ChemSusChem*, **2016**, *9*, 1339-1347.

[S6] Kannapu, H. P. R.; Mullen, C. A.; Elkasabi, Y.; Boateng, A. A. *Fuel Proc. Technol.* **2015**, *137*, 220-228.

[S7] Panagiotopoulou, P.; Martin, N.; Vlachos, D. G. *ChemSusChem*, **2015**, *8*, 2046-2054.

[S8] Li, H.; He, J.; Riisager, A.; Saravanamurugan, S.; Song, B.; Yang, S. *ACS Catal.* **2016**, *6*, 7722-7727.

[S9] Scholz, D.; Aellig, C.; Hermans, I. *ChemSusChem*, **2014**, *7*, 268-275.

Table S2 Detail data of kinetic studies and calculated activation energy for the CTH of FF over NiO(P)-300 ^a

Temp. (K)	1/T (K ⁻¹)	Rate constant k (min ⁻¹)	R ²	Ea (kJ/mol)	R ²
373.15	2.68·10 ⁻³	0.00954	0.99439		
393.15	2.544·10 ⁻³	0.01802	0.98107	41.8	0.99616
413.15	2.42·10 ⁻³	0.03517	0.9307		

^a Reaction conditions: 1 mmol FF, 0.02 g NiO(P)-300, 5 mL 2-propanol, t = 0.5-2.0 h.

Table S3 Catalytic performance of NiO(P)-300 in 2-BuOH at different reaction temperature ^a

Entry	Temp. (°C)	FF conv. (%)	FAOL Yield (%)	FAOL select. (%)
1	120	57.1	56.3	98.6
2	160	89.4	87.4	97.8

^a Reaction conditions: 1 mmol FF, 0.02 g NiO(P)-300, 5 mL 2-BuOH, 3 h.

Table S4. One-pot conversion of FF to IPL with NiO(P)-300 and other acid catalysts ^a

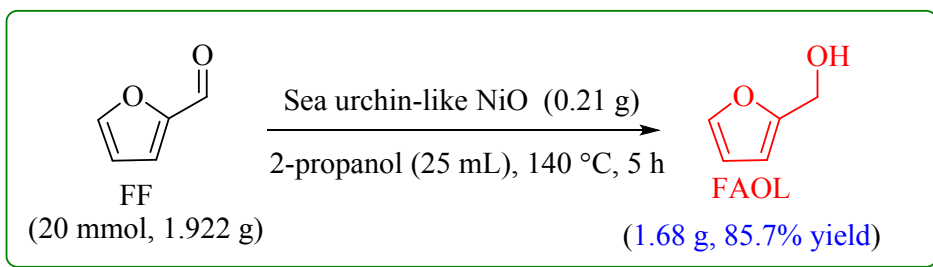
Entry	Acid catalyst	Acid amount (mmol/g) ^b	Conv. (%)	Yield IPL (%)
1	Amberlyst 15	4.7 ^c	>99.9	61.5
2	H-Beta (12.5)	0.86	>99.9	17.0
3	H-ZSM-5 (11.5)	1.49	>99.9	6.8
4	H-MOR (10)	1.77	>99.9	10.8
5	H-Y (6)	0.84	>99.9	30.4

^a Reaction conditions: 1 mmol FF, 0.02 g NiO(P)-300, 0.04 g acid catalyst. One-pot, two-step process where the NiO was removed after 2 h at 140 °C followed by addition of acid catalyst for 4 h at 140 °C. ^b Measured by NH₃-TPD. ^c Measured by acid-base titration.

Table S5. Effect of acid or base additive on the CTH of FF to FAOL over NiO(P)-300 ^a

Entry	Additives	FF Conv. (%)	FAOL Yield (%)	FAOL formation rate ^c ($\mu\text{mol g}^{-1}\text{min}^{-1}$)	TOF ^d (h^{-1})
1	No	72.6	70.2	585	2.6
2	Piperidine ^b	19.5	14.3	119.2	0.53
3	Benzoic acid ^b	11.6	7.4	61.7	0.28

^a Reaction conditions: 1 mmol FF, 5 mL 2-propanol, 0.02 g NiO(P)-300, 120 °C, 1 h. ^b The amount of additives is 0.02 g. ^c Calculated from the yield of GVL obtained after 1 h. ^d Turn-over frequency (TOF) as (mole of FAOL)/(mole of catalyst \times reaction time).



Scheme S1. Gram-scale CTH of FF to FAOL over NiO(P)-300 catalyst.